JNeurosci THE JOURNAL OF NEUROSCIENCE

Research Articles: Behavioral/Cognitive

Establishing the roles of the dorsal and ventral striatum in humor comprehension and appreciation with fMRI

https://doi.org/10.1523/JNEUROSCI.1361-23.2023

Cite as: J. Neurosci 2023; 10.1523/JNEUROSCI.1361-23.2023

Received: 18 July 2023
Revised: 28 September 2023
Accepted: 3 October 2023

Establishing the roles of the dorsal and ventral striatum in humor comprehension and appreciation with fMRI

Abbreviated title: **Dorsal and ventral striatum in humor processing**

Margaret Prenger PhD[a,b,c], Madeline Gilchrist MSc[b,c], Kathryne Van Hedger PhD[a,b,d], Ken N. Seergobin MSc[b], Adrian M. Owen PhD[a,b,e], Penny A. MacDonald MD, PhD[a,b,d]*

[a]BrainsCAN, Western University, London N6A 3K7, Ontario, Canada

[b]Western Institute for Neuroscience, Western University, London N6A 3K7, Ontario, Canada

[c]Department of Neuroscience, Western University, London N6A 3K7, Ontario, Canada

[d]Clinical Neurological Sciences, Schulich School of Medicine & Dentistry, Western University, London N6A 3K7, Ontario, Canada

[e]Departments of Physiology & Pharmacology and Psychology, Western University, London N6A 3K7, Ontario, Canada

***Corresponding Author**

Address: Western University, 1151 Richmond Street, London, Ontario, Canada
Telephone: 519-685-8500 ext. 33631
Email: penny.macdonald@lhsc.on.ca

Number of pages: 41

Number of figures: 6

Number of tables: 5

Number of words (Abstract): 239

Number of words (Introduction): 613

Number of words (Discussion): 1489

Conflict of Interest: The authors declare no competing financial interests.

Acknowledgements: This work was supported by the Canada First Research Excellence Fund awarded to Western University [BrainsCAN]; a Canada Research Chair Tier 2 in Cognitive Neuroscience and Neuroimaging to PAM [950-230372]; and a Canada Institutes of Health Research Project Grant to PAM [R4981A15]. AMO is a Fellow of the CIFAR Brain, Mind, and Consciousness program. The authors would like to thank Dr. Suzanne Witt for her assistance with MRI data organization and preprocessing, and Joe Gati for his input and assistance with scanning protocol development. We also thank MRI Technologists Scott Charlton, Oksana Opalevych, and Trevor Szerkeres for their valuable assistance during data collection.

Abstract

Humor comprehension (i.e., "getting" a joke) and humor appreciation (i.e., enjoying a joke) are distinct, cognitively complex processes. Functional magnetic resonance imaging (fMRI) investigations have identified several key cortical regions but have overlooked subcortical structures that have theoretical importance in humor processing. The dorsal striatum (DS) contributes to working memory, ambiguity processing, and cognitive flexibility – cognitive functions that are required to accurately recognize humorous stimuli. The ventral striatum (VS) is critical in reward processing and enjoyment. We hypothesized that the DS and VS play important roles in humor comprehension and appreciation, respectively. We investigated the engagement of these regions in these distinct processes using fMRI. Twenty-six healthy young male and female human adults completed two humor-elicitation tasks during a 3 Tesla fMRI scan: a traditional behavior-based joke task and a naturalistic audio-visual sitcom paradigm (i.e., *Seinfeld*-viewing task). Across both humor-elicitation methods, whole-brain analyses revealed cortical activation in the inferior frontal gyrus, the middle frontal gyrus, and the middle temporal gyrus for humor comprehension, and the temporal cortex for humor appreciation. Additionally, with region of interest (ROI) analyses, we specifically examined whether DS and VS activation correlated with these processes. Across both tasks, we demonstrated that humor comprehension implicates both the DS and the VS, whereas humor appreciation only engages the VS. These results establish the role of the DS in humor comprehension, which has been previously overlooked, and emphasize the role of the VS in humor processing more generally.

Significance Statement

Humorous stimuli are processed by the brain in at least two distinct stages. First, humor comprehension involves understanding humorous intent through cognitive and problem-solving mechanisms. Second, humor appreciation involves enjoyment, mirth, and laughter in response to a joke. The roles of smaller, subcortical brain regions in humor processing, such as the dorsal striatum (DS) and ventral striatum (VS), have been overlooked in previous investigations. However, these regions are involved in functions that support humor comprehension (e.g., working memory ambiguity resolution, and cognitive flexibility) and humor appreciation (e.g., reward processing, pleasure, and enjoyment). In this study, we used neuroimaging to demonstrate that the DS and VS play important roles in humor comprehension and appreciation, respectively, across two different humor-elicitation tasks.

1 Introduction

Humor is a ubiquitous human experience that serves an adaptive purpose by facilitating social interactions. It is a higher-order ability and requires the integration of multiple cognitive processes. Humor processing can be separated into at least two distinct components: humor comprehension and humor appreciation (Ziv, 1984).

Humor comprehension (i.e., "getting the joke") is a problem-solving process in which one detects and resolves some incongruity or absurdity to reveal the joke (Suls, 1972). Humor appreciation refers to the subjective amusement or mirth experienced upon realizing the joke. Although humor comprehension generally occurs only once, humor appreciation can be experienced repeatedly with further elaboration, explaining why some jokes remain funny even once the punchline is known.

Advances in neuroimaging allow researchers to explore brain regions involved in humor processing. Functional magnetic resonance imaging (fMRI) has revealed many cortical regions as integral to humor processing. Chang and colleagues (2023) identified blood-oxygen-level-dependent (BOLD) activation in the inferior frontal gyrus, the medial frontal gyrus, the superior frontal gyrus, the middle temporal gyrus, and the inferior parietal lobule in incongruity detection and resolution (i.e., humor comprehension). In contrast, activation of the ventromedial prefrontal cortex, the amygdala, the anterior insula, the nucleus accumbens, and the midbrain occurred during the elaboration stage (i.e., humor appreciation). Activation of fronto-temporo-parietal areas during humor comprehension, and of meso-cortico-limbic areas during appreciation aligns with the conclusions of two meta-analyses of 20 and 57 fMRI humor processing studies, respectively (Farkas et al., 2021; Vrticka et al., 2013).

The role of the dorsal striatum (DS; i.e., dorsal caudate nucleus and putamen) in humor processing has generally been overlooked. Although activations of the left putamen (Filik et al., 2019; Iwase et al., 2002; Sanz-Arigita et al., 2021), the right putamen (Goldin et al., 2005; Neely et al., 2012; Shibata et al., 2014), the left caudate (Sanz-Arigita et al., 2021), and the right caudate (Goldin et al., 2005; Osaka et al., 2014; Sanz-Arigita et al., 2021) have been identified in studies of humor processing, most authors do not put importance on these findings or discuss their implications. Filik and colleagues (2019) were the lone authors to discuss the putamen's role in language processing and how this could contribute to humor comprehension. The DS's involvement in ambiguity resolution (Crinion et al., 2006; MacDonald and Monchi, 2011; Mestres-Missé et al., 2012), suppression of pre-potent responses (Akkermans et al., 2018; MacDonald and Monchi, 2011; Zandbelt and Vink, 2010), working memory (Darvas et al., 2014; Lewis et al., 2004; MacDonald and Monchi, 2011), and set-shifting (Darvas et al., 2014; MacDonald and Monchi, 2011), which are essential for humor comprehension, have not been considered in the context of humor processing. The tendency is to ignore these DS activations or explain them in the context of reward processing, though experiencing humorous stimuli as rewarding pertains to humor appreciation, a process that has been shown clearly to implicate the ventral striatum (VS; nucleus accumbens and ventral caudate nucleus and putamen, $z \leq 2$ using MRI; Azim et al., 2005; Mobbs et al., 2005, 2003; Neely et al., 2012; Noh et al., 2014; Shibata et al., 2014; Watson et al., 2007) and not the DS. Discounting the DS's role in cognitive functions and misattributing all striatal activations in humor processing to affective/reward functions has caused sub-regions of the striatum to be excluded in reviews of the literature and theories of humor processing.

Our aim was to directly investigate the distinct contributions of the DS and VS in humor processing. We predicted that humor comprehension will involve the DS whereas humor appreciation will engage the VS. We investigated these hypotheses using both a traditional behavior-based humor processing task and a naturalistic sitcom-viewing method in fMRI with striatal ROIs.

2 Materials and Methods

2.1 Participants

Twenty-six young, healthy individuals participated in this study (11 male; $M_{\text{age}} = 22.35$, $SD_{\text{age}} = 3.43$; $M_{\text{education}} = 16.40$, $SD_{\text{education}} = 2.61$). All participants had normal or corrected-to-normal vision, had no history of neurological or psychiatric disorders, and did not abuse drugs or alcohol at the time of participation. All participants provided informed consent according to the Declaration of Helsinki (World Medical Association, 2013) and all procedures were approved by the Research Ethics Board at the University of Western Ontario (London, Ontario, Canada).

2.2 Experimental Design

2.2.1 Joke Task

Participants completed a humor processing task (i.e., Joke task) that involved listening to 40 randomly-selected audio clips of jokes out of a possible bank of 80 stimuli, as well as 40 randomly-selected audio clips of neutral, non-joke sentences, out of a possible bank of 80 stimuli, while neural activity was measured using fMRI. The majority of these audio clip stimuli (92 out of 160) were used in previous studies (Bekinschtein et al., 2011; Fiacconi and Owen, 2015), and joke and non-joke stimuli were presented in random order. All audio clip stimuli were recorded in a male voice and spoken neutrally, so as not to reveal whether the audio clip was a joke or non-joke based on intonation or prosody. The audio was presented through MRI-compatible headphones. A short movie clip was played to participants in the scanner, prior to the onset of the experimental task to ensure that participants could hear through both headphones and that the volume was appropriate.

Following the presentation of each audio clip, participants were asked to indicate whether they thought the audio clip was a joke, or not a joke. For all stimuli (jokes and non-jokes), they were also asked to rate how funny they found each audio clip on a scale from 1 (not funny at all) to 4 (extremely funny). Inter-trial and inter-response intervals were jittered with variable durations sampled from an exponential distribution (min = 525 msec; mean = 2500 msec; max = 7000 msec). Participants used a handheld Current Designs 4-button fiber optic response pad (HHSC-1x4-L) to make their responses by moving a green selection highlight up (index finger – Button 2) or down (middle finger – Button 3) and confirming their response (ring finger – Button 4). The starting position of the green highlighted selection was randomized on each response screen to mitigate biases in response times (RT) for selections that were closer or further to the starting position. Participants had a maximum of 5000 msec for each response (List of Figures

Figure). Prior to completing the task, all participants watched a video containing detailed instructions of the procedure. Participants were provided an opportunity to ask questions for further clarification, if necessary.

2.2.2 *Seinfeld*-viewing Task

Immediately following the humor processing task, participants were shown a full episode of the sitcom *Seinfeld*. Half of the participants were shown the episode "The Airport" (Cherones, 1992). The other half of participants were shown the episode "The Movie" (Cherones, 1993). These specific episodes were selected due to their relative lack of overt racial and sexual humor and their focus on common activities that most individuals have previously experienced (i.e., traveling in an airplane and going to the movie theater). The episodes were visually projected onto a screen at the end of the magnet bore, which participants viewed through a mirror. Participants were instructed to watch and listen to the episode, refrain from falling asleep, and be prepared to answer questions pertaining to the clip after the episode.

Following the episode and outside of the scanner, participants completed a questionnaire which evaluated their prior familiarity with *Seinfeld*, how frequently they watched sitcoms and funny television in general, how funny they found the episode of *Seinfeld*, and some true/false questions about the episode's plot to ensure that they had indeed attended to the episode.

2.3 **Imaging Acquisition**

All imaging data were collected on a 3 Tesla Siemens Magnetom Prisma Fit MRI scanner at the Centre for Functional and Metabolic Mapping (CFMM) located in the Robarts Research Institute at the University of Western Ontario. Data were acquired using a 32-channel head coil.

First, a localizer image was obtained to identify the optimal scanning area relative to the participant's head position. Separate T2*-weighted multiband echo-planar imaging (EPI) functional scans were acquired during the humor processing task and the *Seinfeld* episode with the following parameters: repetition time (TR) = 1000 msec, echo time (TE) = 30 msec, 48 slices oriented along the anterior and posterior commissure with 2.5 mm thickness, flip angle = 40°, field of view (FOV) = 220 x 220 mm^2, voxel size = 2.5 x 2.5 x 2.5 mm^3, multiband factor = 4. Finally, a T1-weighted (T1w) MPRAGE anatomical scan was acquired with the following parameters: TR = 2400 msec, TE = 2.28 msec, 192 sagittal slices with 0.80 mm thickness, flip angle = 8°, FOV = 256 x 256 mm^2, voxel size = 0.8 x 0.8 x 0.8 mm^3.

2.4 Imaging Preprocessing

Results included in this manuscript were achieved through image preprocessing performed using *fMRIPrep* 1.5.4 (Esteban, Markiewicz, et al., 2018); (Esteban, Blair, et al., 2018); RRID:SCR_016216), which is based on *Nipype* 1.3.1 (Gorgolewski et al., 2011); (Gorgolewski et al., 2018); RRID:SCR_002502). Visualization of fMRI data was conducted with MRIcroGL (v. 13.1; Rorden and Brett, 2000).

2.4.1 Anatomical Data Preprocessing

The T1w image was corrected for intensity non-uniformity (INU) with N4BiasFieldCorrection (Tustison et al., 2010), distributed with ANTs 2.2.0 (Avants et al., 2008; RRID:SCR_004757), and used as T1w-reference throughout the workflow. The T1w-reference was then skull-stripped with a *Nipype* implementation of the antsBrainExtraction.sh workflow (from ANTs), using OASIS30ANTs as target template. Brain tissue segmentation of cerebrospinal fluid (CSF), white-matter (WM) and gray-matter (GM) was performed on the brain-extracted T1w using fast (FSL 5.0.9; RRID:SCR_002823; Zhang et al., 2001). Brain surfaces were reconstructed using recon-all (FreeSurfer 6.0.1, RRID:SCR_001847; Dale et al., 1999), and the brain mask estimated previously was refined with a custom variation of the method to reconcile ANTs-derived and FreeSurfer-derived segmentations of the cortical gray-matter of Mindboggle (RRID:SCR_002438, Klein et al., 2017). Volume-based spatial normalization to one standard space (MNI152NLin2009cAsym) was performed through nonlinear registration with antsRegistration (ANTs 2.2.0), using brain-extracted versions of both T1w reference and the T1w template. The following template was selected for spatial normalization: *ICBM 152 Nonlinear Asymmetrical template version 2009c* (Fonov et al., 2009, RRID:SCR_008796; TemplateFlow ID: MNI152NLin2009cAsym).

2.4.2 Functional Data Preprocessing

For each of the BOLD runs found per subject (across both tasks), the following preprocessing was performed. First, a reference volume and its skull-stripped version were generated using a custom methodology of *fMRIPrep*. A B0-nonuniformity map (or *fieldmap*) was estimated based on a phase-difference map calculated with a dual-echo GRE (gradient-recall echo) sequence, processed with a custom workflow of *SDCFlows* inspired by the epidewarp.fsl script and further improvements in HCP Pipelines (Glasser et al., 2013). The *fieldmap* was then co-registered to the target EPI (echo-planar imaging) reference run and converted to a displacements field map (amenable to registration tools such as ANTs) with FSL's fugue and other *SDCflows* tools. Based on the estimated susceptibility distortion, a corrected EPI (echo-planar imaging) reference was calculated for a more accurate co-registration with the anatomical reference. The BOLD reference was then co-registered to the T1w reference using bbregister (FreeSurfer) which implements boundary-based registration (Greve and Fischl, 2009). Co-registration was configured with six degrees of freedom. Head-motion parameters with respect to the BOLD reference (transformation matrices, and six corresponding rotation and translation parameters) are estimated before any spatiotemporal filtering using mcflirt (FSL 5.0.9, Jenkinson et al., 2002). BOLD runs were slice-time corrected using 3dTshift from AFNI 20160207 (Cox and Hyde, 1997), RRID:SCR_005927). The BOLD time-series were resampled to surfaces on the following spaces: *fsaverage5*. The BOLD time-series (including slice-timing correction when applied) were resampled onto their original, native space by applying a single, composite transform to correct for head-motion and susceptibility distortions. These resampled BOLD time-series will be referred to as *preprocessed BOLD in original space*, or just *preprocessed BOLD*. The BOLD time-series were resampled into standard space, generating a *preprocessed BOLD run in ['MNI152NLin2009cAsym'] space*. First, a reference volume and its skull-stripped version were generated using a custom methodology of *fMRIPrep*. Several confounding time-series were calculated based on the *preprocessed BOLD*: framewise displacement (FD), DVARS and three region-wise global signals. FD and DVARS are calculated for each functional run, both using their implementations in *Nipype* (following the definitions by Power et al., 2014). The three global signals are extracted within the CSF, the WM, and the whole-brain masks. Additionally, a set of physiological regressors were extracted to allow for component-based noise correction (*CompCor*, Behzadi et al., 2007). Principal components are estimated after high-pass filtering the *preprocessed BOLD* time-series (using a discrete cosine filter with 128s cut-off) for the two *CompCor* variants: temporal (tCompCor) and anatomical (aCompCor). tCompCor components are then calculated from the top 5% variable voxels within a mask covering the subcortical regions. This subcortical mask is obtained by heavily eroding the brain mask, which ensures it does not include cortical GM regions. For aCompCor, components are calculated within the intersection of the aforementioned mask and the union of CSF and WM masks calculated in T1w space, after their projection to the native space of each functional run (using the inverse BOLD-to-T1w transformation). Components are also calculated separately within the WM and CSF masks. For each CompCor decomposition, the *k* components with the largest singular values are retained, such that the retained components' time series are sufficient to explain 50 percent of variance across the nuisance mask (CSF, WM, combined, or temporal). The remaining components are dropped from consideration. The head-motion estimates calculated in the correction step were also placed within the corresponding confounds file. The confound time series derived from head motion estimates and global signals were expanded with the inclusion of temporal derivatives and quadratic terms for each (Satterthwaite et al., 2013).

Frames that exceeded a threshold of 0.5 mm FD or 1.5 standardised DVARS were annotated as motion outliers. All resamplings can be performed with *a single interpolation step* by composing all the pertinent transformations (i.e., head-motion transform matrices, susceptibility distortion correction when available, and co-registrations to anatomical and output spaces). Gridded volumetric resamplings were performed using antsApplyTransforms (ANTs), configured with Lanczos interpolation to minimize the smoothing effects of other kernels (Lanczos, 1964). Non-gridded surface resamplings were performed using mri_vol2surf (FreeSurfer). Many internal operations of *fMRIPrep* use *Nilearn* 0.6.0 (Abraham et al., 2014, RRID:SCR_001362), mostly within the functional processing workflow. For more details of the pipeline, see the section corresponding to workflows in *fMRIPrep*'s documentation. Following this preprocessing pipeline, the normalized data were spatially smoothed with an 8mm full-width half-maximum Gaussian kernel using SPM12.

2.5 Statistical Analysis

Demographic and behavioral data were analyzed with R statistical computing software (v. 4.2.0; R Core Team, 2022)) and R Studio (v. 2022.07.01; RStudio Team, 2022). Data were examined for outliers above or below 3 x the interquartile range (IQR). RT data for both humor comprehension and appreciation were also examined for time-out instances, in which participants failed to respond within the 5-second time limit.

2.5.1 Imaging Analysis

fMRI data were analyzed using Statistical Parametric Mapping version 12 software (SPM12; Wellcome Department of Imaging Neuroscience, 2014) and MATLAB (v. R2022a; The Mathworks Inc., 2022).

2.5.1.1 Joke Task fMRI Analysis

Separate first-level, fixed-effects analyses were performed for each individual participant. For humor comprehension, a general linear model (GLM) was constructed in which the canonical hemodynamic response function was convolved with the onsets and durations of the auditory stimuli for each stimulus category. Only the trials in which the participant correctly identified the stimulus as either a joke or a non-joke were included in this GLM. Two regressors of interest were included in the model: 1) Jokes, and 2) Non-Jokes. Average cerebrospinal fluid (CSF) signal, global signal, and the six head motion parameters (translation and rotation in x, y, and z dimensions) were included as covariates of no interest. Following model estimation, a single contrast of interest was examined: the main effect of Joke (i.e., Joke > Non-Joke). For humor appreciation, a separate GLM was constructed in which two regressors of interest were modeled: 1) Funny (i.e., trials on which participants' funniness ratings equaled or exceeded 2), and 2) Not Funny (i.e., trials on which that participants' funniness ratings equaled 1), along with average CSF, global signal, and the six head motion parameters as covariates of no interest. All trials were analyzed. A single contrast of interest was examined: the main effect of Funny (Funny > Not Funny).

Next, second-level random effects analyses were conducted. Contrast images from each participant were examined in separate group-level *t*-tests for each main and interaction effect. Consistent with previous humor processing literature, whole-brain analyses were examined using a conservative voxel-level FWE-corrected height threshold of $p < 0.05$ and a cluster-level extent threshold of $k = 10$ consecutive voxels. The anatomical location of the peak voxel within each cluster that survived this threshold was identified using the automated anatomical labelling atlas 3 (AAL3; Rolls et al., 2020).

To specifically test our hypothesis that the striatum is involved in humor processing, regions of interest (ROIs) were generated using MarsBaR (Brett et al., 2002) based on those described in Hiebert et al. (2019). Briefly, the DS ROI contained the bilateral dorsal caudate nucleus and the bilateral dorsal putamen at a level of $z > 2$ mm in MNI space. The VS ROI contained the bilateral nucleus accumbens, bilateral ventral caudate nucleus, and bilateral ventral putamen at a level of $z \leq 2$ mm in MNI space. The $z = 2$mm cut-off was based on a review by Postuma and Dagher (2006). These ROIs are depicted in MNI space in **Error! Reference source not found.**. For each contrast of interest, average beta values for DS and VS ROIs were estimated and compared to zero with Bonferroni-corrected one-sample *t*-tests. In the case of non-significant results, support in favor of the null hypothesis was examined with Bayesian analysis (Dienes, 2014; Keysers et al., 2020). The magnitude of the resulting Bayes Factor (BF_{10}), a ratio of evidence for or against a null hypothesis, was evaluated compared to the cut-offs suggested by Jeffreys (1939), in which a $BF_{10} > 3$ represents substantial evidence in favor of the alternative hypothesis.

2.5.1.2 *Seinfeld*-viewing Task fMRI Analysis

Our *Seinfeld* viewing paradigm was modeled upon the study of Moran and colleagues (2004). As shown in Figure, the laugh track of each episode was used to create event epochs for a) humor comprehension, defined as the two seconds prior to the onset of the laugh track, b) humor appreciation, specified as the middle two seconds of laughter in the laugh track, and c) control, characterized as the two second period occurring midway between the end of the last humor appreciation event and the next humor comprehension event. Laugh track epochs were identified by four independent raters. The resulting event onsets and durations for each condition were based on the consensus of these raters and confirmed by visual inspection of the audio waveform of the episode.

As opposed to the Joke task, which uses “canned” jokes that are rarely encountered in everyday life, the *Seinfeld*-viewing task represents a uniquely naturalistic approach to evaluating humor comprehension and appreciation. However, it is important to note that the humor comprehension and appreciation events in the *Seinfeld*-viewing task are not participant-driven like those of the Joke task are. The humor comprehension and appreciation events in the *Seinfeld*-viewing task are based on the moments of the episode(s) that a live studio audience from the 1990s found to be funny, which might not necessarily represent the moments of the episode(s) that our participants found to be funny.

First-level, fixed-effects analyses were performed for each individual participant. For humor comprehension, a GLM was constructed, convolving the canonical hemodynamic response function with the onsets and durations of the comprehension and control events. These events were used as regressors of interest along with the CSF signal, global signal, and six head motion parameters as covariates of no interest. Following model estimation, a single contrast of interest was examined: the main effect of humor comprehension (i.e., humor comprehension > control). For humor appreciation, a separate GLM was constructed, in which a single contrast of interest was examined: the main effect of humor appreciation (i.e., humor appreciation > control). We considered activations during this contrast to be attributable to the experience of humor appreciation, as opposed to a reaction to hearing others laugh, given that Moran et al. (2004) observed nearly identical activations for humor appreciation across their two separate sitcom-viewing fMRI experiments that did and did not include a laugh track.

Next, second-level random effects analyses were conducted. Contrast images from each participant were examined in separate group-level *t*-tests for each main and interaction effect. Consistent with the *Seinfeld*-viewing study by (Moran et al., 2004), whole-brain analyses were examined. However, we used a more conservative voxel-level FWE-corrected height threshold of $p < 0.05$ and a cluster-level extent threshold of $k = 10$ consecutive voxels. The anatomical location of the peak voxel within each cluster that survived this threshold was identified using the AAL3 (Rolls et al., 2020). To specifically test our hypothesis that the striatum is involved in humor processing, we used the same DS and VS ROIs as described above. For each contrast of interest, average beta values for DS and VS ROIs were estimated and included in the analyses.

2.5.2 Conjunction Analysis

To determine which regions are jointly activated during our contrasts of interest between the Joke task and the *Seinfeld*-viewing task for humor comprehension and humor appreciation, we conducted conjunction analyses using the procedure suggested by Nicols et al. (2005).

3 Results

3.1 Behavioral Results

3.1.1 Joke Task: Humor Comprehension

Humor comprehension was calculated as the percentage of correctly identified joke and non-joke stimuli. These data were entered into a paired *t*-test. The difference in humor comprehension accuracy between jokes and non-jokes did not reach significance ($t(51) = -1.87$, $p = 0.068$), with Joke stimuli ($M = 86.06\%$, 95% CI [82.22, 89.89]) being slightly more accurately categorized than Non-Joke stimuli ($M = 81.35\%$, 95% CI [82.22, 89.89]).

3.1.2 Joke Task: Humor Appreciation

Humor appreciation was calculated as the average funniness ratings of joke and non-joke stimuli. These data were entered into a paired *t*-test. Unsurprisingly, there was a significant difference in funniness estimates between jokes and non-jokes ($t(51) = -18.54$, $p < 0.001$). There was also a significant positive correlation between funniness ratings for joke stimuli and SHQ-6 scores ($r = 0.29$, $p = 0.03$), suggesting that participants with a greater sense of humor tended to rate joke stimuli as funnier.

3.1.3 *Seinfeld*-viewing Task: Post-Scan Questionnaire

A chi-squared test of independence was conducted to examine the proportion of individuals in each episode group who had never watched a single episode of Seinfeld to those who had prior experience with the show. There was not a significant difference in the familiarity with *Seinfeld* ($\chi^2 = 0.62$, $p = 0.43$) between participants assigned to the different Seinfeld episodes. Finally, a two-sample *t*-test evaluated the difference in mean funniness rating accorded to each episode of *Seinfeld* by the participants who watched “The Airport” and “The Movie” respectively. There was no significant difference in funniness ratings between the episodes ($t(24) = -1.17$, $p = 0.26$). Taken together, the two episodes of *Seinfeld* and the groups of participants who viewed each episode respectively, were deemed equivalent. All subsequent analyses were conducted on data collapsed across the groups of participants who viewed different episodes of *Seinfeld* groups. All post-scanning questionnaire data are shown in Table 1.

3.2 Whole-Brain fMRI Results

3.2.1 Joke Task: Humor Comprehension

Significant activations for the contrast of interest pertaining to humor comprehension (Joke > Non-Joke) are listed in Table 2. Only trials in which stimuli were correctly categorized as either jokes or non-jokes were analyzed. Clusters that contain striatal or midbrain structures are marked in Table 2.

3.2.2 Joke Task: Humor Appreciation

There were no significant differences in head motion during funny and not funny trials, as evaluated by Bonferroni-corrected paired *t*-tests for each of the 6 head motion parameters. Significant activations for the humor appreciation contrast are listed in Table 3. Again, clusters that contain striatal or midbrain structures are marked in Table 3.

3.2.3 *Seinfeld*-viewing Task: Humor Comprehension

Moments of humor comprehension were defined as the two second epochs immediately preceding the onset of laughter in the laugh track of *Seinfeld* and were contrasted to two second control epochs selected from the midpoint between the offset and onset of consecutive laugh track epochs. Significant activations for the humor comprehension contrast are listed in Table 4. Clusters that contain striatal or midbrain structures are marked in Table 4.

3.2.4 *Seinfeld*-viewing Task: Humor Appreciation

Moments of humor appreciation were defined as the middle two seconds of laughter in the laugh track of *Seinfeld* and were contrasted to the same two second control epochs selected from the midpoint of consecutive laugh track epochs, as described above. For each of the six head motion parameters, Bonferroni-corrected paired *t*-tests were conducted to compare motion during humor appreciation events to control events. Importantly, none were significant, suggesting that there was no difference in the amount of head motion during laugh track epochs compared to the remainder of the episode. Significant activations for the humor appreciation contrast are listed in Table 5. Clusters that contain striatal or midbrain structures are marked in Table 5.

3.2.5 Conjunction Analyses

Brain regions that were significantly activated across tasks for the humor comprehension and humor appreciation contrasts were identified using conjunction analyses. For the humor comprehension contrasts, regions that were significantly activated across tasks included the left inferior frontal gyrus, the bilateral middle frontal gyrus, the bilateral middle temporal gyrus, the bilateral temporal poles, the right fusiform gyrus, the left supplementary motor area, the left angular gyrus and the right supramarginal gyrus (i.e., the inferior parietal lobule), the left insula, the right red nucleus, the left thalamus, and the bilateral amygdala. Regions that were commonly activated by the humor appreciation contrasts across tasks included the left middle frontal gyrus, the left superior frontal gyrus, the bilateral middle temporal gyrus, the bilateral temporal poles, the right superior parietal lobule, the left angular gyrus, the right supramarginal gyrus, the left precuneus, the left lingual gyrus, the right cuneus, and the left thalamus. Activation maps of both conjunction analyses can be viewed in Figure 4.

3.3 Striatal ROI Results

Significant activations in the DS and VS ROIs are presented at a level of $p < 0.05$, corrected for multiple comparisons with the Bonferroni method.

3.3.1 Joke Task: Humor Comprehension

As we did previously in the whole-brain analyses, humor comprehension was evaluated in the Joke task by the Joke > Non-Joke contrast for correct trials only. To determine whether the DS and/or VS contribute to humor comprehension, average activation during this contrast in the DS and VS ROIs was compared to zero using separate one-sample *t*-tests, corrected for multiple comparisons. We observed activation that was significantly different from zero in both the DS ($t(25) = 2.94$, $p = 0.014$) and the VS ($t(25) = 3.99$, $p = 0.001$) ROIs (Figure 5A) during humor comprehension in the Joke task.

3.3.2 Joke Task: Humor Appreciation

For humor appreciation, we evaluated average activation in the DS and VS ROIs for the Funny > Not Funny contrast (calculated for all trials). This activation was compared to zero in separate one-sample *t*-tests for each ROI. We observed significant activation in the VS ($t(25) = 3.00$, $p = 0.012$), but not in the DS ($t(25) = 2.04$, $p = 0.10$; Figure 5B) for humor appreciation. Evaluation of this null effect using a Bayesian one-sample *t*-test with default effect size priors (Cauchy scale 0.707) suggested that there was a lack of evidence supporting DS activation during moments of humor appreciation ($BF_{10} = 1.22$).

3.3.3 *Seinfeld*-viewing Task: Humor Comprehension

For humor comprehension in the *Seinfeld*-viewing task, we calculated the average activation in the DS and VS during the 2-seconds prior to the onset of laughter in the episode laugh track, compared to control epochs of equal duration sampled from the rest of the episode. This activation was compared to zero with separate one-sample *t*-tests, corrected for multiple comparisons. We observed activation that was significantly different from zero in both the DS ($t(25) = 3.53$, $p = 0.003$) and the VS ($t(25) = 2.79$, $p = 0.02$) ROIs (Figure 6A).

3.3.4 *Seinfeld*-viewing Task: Humor Appreciation

For humor appreciation in the *Seinfeld*-viewing task, we calculated the average activation in the DS and VS during the middle 2-seconds of laugh-track laughter, compared to control epochs of equal duration selected from the remainder of the episode. This activation was compared to zero with separate one-sample *t*-tests for each ROI, corrected for multiple comparisons. We observed activation that was significantly different from zero in the VS ($t(25) = 2.94$, $p = 0.014$) ROI, but not in the DS ($t(25) = 1.81$, $p = 0.016$), as shown in Figure 6B. To evaluate the strength of evidence for the hypothesis that the DS is activated during humor appreciation, a Bayesian one-sample *t*-test was conducted using default effect size priors (Cauchy scale 0.707). There was no support for this alternative hypothesis ($BF_{10} = 0.86$), suggesting that the DS does not play a role in humor appreciation.

4 Discussion

Using fMRI and two independent measures of humor processing, performed by the same healthy young participants, we investigated BOLD activity associated with humor comprehension and humor appreciation. In whole-brain analyses, for both tasks, we found significant activation of the inferior frontal gyrus, the middle frontal gyrus, the supplementary motor area, the middle temporal gyrus, the temporal poles, and the midbrain for humor comprehension. We found common activations in the temporal cortex (i.e., BA 37 and BA 38) for humor appreciation in both tasks. In addition to whole-brain analyses, we examined BOLD signal in the DS and VS associated with humor comprehension and appreciation with an ROI approach. In both tasks, we found that humor comprehension seems to implicate both the DS and VS, whereas humor appreciation preferentially engages the VS. These findings align with our expectations that different brain regions underlie humor comprehension and appreciation and that the striatum is involved in humor processing.

Our whole-brain and conjunction analyses corroborated the findings of previous studies regarding cortical regions that are involved in humor comprehension and appreciation. For the humor comprehension contrast in the Joke task, we found significant activation in the left inferior frontal gyrus, the left middle frontal gyrus, the left superior frontal gyrus, the bilateral middle temporal gyrus, the bilateral temporal pole, the left angular gyrus, the left supplementary motor area, the left precentral gyrus, the left putamen, the left midbrain, the left thalamus, and the right amygdala. We corroborated these results with our *Seinfeld*-viewing task, albeit with a slight shift in hemispheric lateralization, finding significant clusters of activation in the left inferior frontal gyrus, the right middle frontal gyrus, the bilateral middle temporal gyrus, the right superior temporal gyrus, the right temporal pole, the right supramarginal gyrus, the left fusiform gyrus, the right supplementary motor area, the bilateral insula, the left hippocampus, the left midbrain, and the right amygdala. Many of these cortical regions (e.g., the inferior frontal gyrus, the middle temporal gyrus) have been identified in previous studies of humor comprehension (Bartolo et al., 2000; Bekinschtein et al., 2011; Chan et al., 2013; Goel and Dolan, 2001; Osaka et al., 2014; Samson et al., 2009, 2008; Vrticka et al., 2013; Wild et al., 2006). The shift in hemispheric lateralization between the Joke task and *Seinfeld*-viewing might be due to the differences in humor modality between these tasks. Verbal humor, which was measured in the Joke task, is associated with greater activation in the left hemisphere, whereas visual/situational humor as assessed in the *Seinfeld*-viewing task, is associated with greater activation in the right hemisphere (Moran et al., 2004; Vrticka et al., 2013). We also found activation in a cluster encompassing the left putamen in this contrast, which is consistent with a recent meta-analysis of 28 studies that identified co-activation of the left anterior putamen and cortical regions such as the inferior frontal gyrus and precentral gyrus during language processing tasks (Viñas-Guasch and Wu, 2017). Finally, we also observed significant activation of the left midbrain for humor comprehension in both tasks, which, coupled with our striatal ROI findings, could indicate that humor comprehension involves dopamine signaling. For humor appreciation, we found activations of BA 38 (temporal pole) in the Joke task and BA 37 (inferior temporal gyrus) in the *Seinfeld*-viewing task. Our conjunction analysis confirmed that temporal regions, among others, were activated by humor appreciation across both tasks. The temporal cortex has been implicated in laughter associated with mirth (Caruana et al., 2015; Satow et al., 2003; Swash, 1972; Wildgruber et al., 2013; Yamao et al., 2015), as opposed to non-mirthful laughter which implicates the anterior cingulate cortex (Caruana et al., 2015), a region which was not identified in our whole-brain analyses of humor appreciation. Importantly, the temporal cortex has been identified in previous fMRI studies of humor appreciation (Amir et al., 2015; Kipman et al., 2012; Mobbs et al., 2003). Interestingly, our humor appreciation conjunction analysis also revealed activation of medial occipital regions (i.e., the lingual gyrus and the cuneus). These regions have been implicated in non-visual functions such as language processing (Palejwala et al., 2021).

Consistent with other studies of humor processing, our whole-brain analyses showed sparse subcortical activation. Although whole-brain analysis is a popular approach for analyzing fMRI data, the height- and extent-thresholds that are routinely applied to correct for multiple comparisons favor larger cortical regions, making it difficult for activation in small brain regions (e.g., DS and VS) to survive these corrections. Illustrating this, most of our striatal and midbrain clusters barely exceed 10 contiguous voxels, with our largest measuring only 112 voxels in extent. Failing to account for these small-volume regions either through ROI analyses or small-volume correction might have led to omission of the striatum and midbrain in theories of humor processing.

For our striatal ROI analyses, we found significant activation in the DS and VS for humor comprehension in both the Joke and *Seinfeld*-viewing tasks. This supports and extends our initial hypothesis that the DS is involved in humor comprehension. Firstly, the DS is implicated in cognitive functions that underlie humor comprehension, including inhibition of prepotent responses (Akkermans et al., 2018; MacDonald and Monchi, 2011; Zandbelt and Vink, 2010), cognitive flexibility (Crinion et al., 2006; MacDonald and Monchi, 2011; Mestres-Missé et al., 2012), and working memory (Darvas et al., 2014; Lewis et al., 2004; MacDonald and Monchi, 2011). Furthermore, the DS is functionally and structurally connected to frontotemporal cortical regions that have been implicated in humor comprehension and related processes, such as the inferior frontal gyrus (Graff-Radford et al., 2017; Haber, 2016; Kireev et al., 2015). For example, the right putamen demonstrates functional connectivity with the left inferior frontal gyrus, the left superior temporal gyrus, the left precentral gyrus, and the left middle temporal gyrus during language processing (Viñas-Guasch and Wu, 2017) and the left caudate head and the inferior frontal gyrus demonstrate increased functional connectivity during deliberate deception in young, healthy humans (Kireev et al., 2015). Finally, there is evidence that patients with Parkinson's disease, in which the DS is dopamine-depleted, experience deficits in humor comprehension but not humor appreciation (Prenger et al., under review). Taken together, this body of literature supports the notion that the DS is intricately involved in social and cognitive functions, such as humor comprehension, via its connections with cortical areas that have a demonstrated role in humor comprehension. Here, we have demonstrated that the DS indeed plays a role in humor comprehension and have replicated this result across two different humor processing elicitation methods.

The involvement of the VS in humor comprehension was somewhat unanticipated. There are a few studies that implicate the VS, and the ventral tegmental area (VTA; region that supplies dopamine to the VS), in humor comprehension (Chan et al., 2012, 2023). It is possible that the VS contributes to humor comprehension by motivating the resolution of incongruities. In their discussion, Chan and colleagues (2012) suggest that VS activation during humor comprehension might be related to a feeling of relief associated with incongruity resolution that might be separate from the amusement feeling of humor appreciation. The VS is also implicated in reward expectation (de la Fuente-Fernández et al., 2002; Filimon et al., 2020; Knutson et al., 2001; Pool et al., 2022). Given that humor comprehension is an effortful process, activation of the VS in anticipation of a potential humor appreciation-related reward might help to drive the humor comprehension process forward. This could be related to the role of the VS in humor generation (another effortful process), demonstrated by Amir & Biederman (2016).

Unsurprisingly, we observed significant activation of the VS during humor appreciation in the Joke task and the *Seinfeld*-viewing task. Activation of the VS during humor appreciation has been well-established in previous literature (Azim et al., 2005; Bekinschtein et al., 2011; Chang et al., 2023; Mobbs et al., 2003, 2005; Neely et al., 2012; Noh et al., 2014; Shibata et al., 2014; Watson et al., 2007), and aligns with the role of the VS in reward processing and prediction error (Schultz, 2016). Importantly, our Bayesian one-sample *t*-tests supported the null hypothesis that the DS is not activated during humor appreciation. DS activation during humor processing appears not to be linked to the rewarding nature of humor appreciation. Rather, activation of the DS during humor processing seems related to the cognitive processes that support humor comprehension.

Our findings represent an advancement in the field of humor research by establishing roles for both the DS and VS in humor comprehension, and for the VS only in humor appreciation. This could suggest that midbrain dopaminergic signaling is an important component of humor processing. So far, only behavioral research has demonstrated humor comprehension deficits in dopamine-related disorders, such as Parkinson's disease (Benke et al., 1998; Mensen et al., 2014; Prenger et al., under review; Thaler et al., 2012). Further research using neuroimaging, clinical cohorts, and pharmacological manipulation would provide further support for the hypothesis that dopamine signaling is involved in humor comprehension and appreciation.

References

Abraham, A., Pedregosa, F., Eickenberg, M., Gervais, P., Mueller, A., Kossaifi, J., Gramfort, A., Thirion, B., & Varoquaux, G. (2014). Machine learning for neuroimaging with scikit-learn. *Frontiers in Neuroinformatics*, *8*. https://doi.org/10.3389/fninf.2014.00014

Akkermans, S. E. A., Luijten, M., van Rooij, D., Franken, I. H. A., & Buitelaar, J. K. (2018). Putamen functional connectivity during inhibitory control in smokers and non-smokers. *Addiction Biology*, *23*(1), 359–368.

Amir, O., Biederman, I., Wang, Z., & Xu, X. (2015). Ha ha! versus aha! A direct comparison of humor to nonhumorous insight for determining the neural correlates of mirth. *Cerebral Cortex* , *25*(5), 1405–1413.

Amir, O., & Biederman, I. (2016). The neural correlates of humor creativity. *Frontiers in Human Neuroscience*, *10*, 597. https://doi.org/10.3389/fnhum.2016.00597

Avants, B. B., Epstein, C. L., Grossman, M., & Gee, J. C. (2008). Symmetric diffeomorphic image registration with cross-correlation: Evaluating automated labeling of elderly and neurodegenerative brain. *Medical Image Analysis*, *12*(1), 26–41.

Azim, E., Mobbs, D., Jo, B., Menon, V., & Reiss, A. L. (2005). Sex differences in brain activation elicited by humor. *Proceedings of the National Academy of Sciences of the United States of America*, *102*(45), 16496–16501.

Bartolo, A., Benuzzi, F., Nocetti, L., Baraldi, P., & Nichelli, P. (2000). Humor comprehension and appreciation: An fMRI study. *Neuroimage*, *11*, 157–166.

Behzadi, Y., Restom, K., Liau, J., & Liu, T. T. (2007). A component based noise correction method (CompCor) for BOLD and perfusion based fMRI. *NeuroImage*, *37*(1), 90–101.

Bekinschtein, T. A., Davis, M. H., Rodd, J. M., & Owen, A. M. (2011). Why clowns taste funny: The relationship between humor and semantic ambiguity. *The Journal of Neuroscience: The Official Journal of the Society for Neuroscience*, *31*(26), 9665–9671.

Benke, T., Bösch, S., & Andree, B. (1998). A study of emotional processing in Parkinson's disease. *Brain and Cognition*, *38*(1), 36–52.

Brett, M., Anton, J.-L., Valabregue, R., & Poline, J.-B. (2002). Region of interest analysis using an SPM toolbox [abstract]. *8th International Conference on Functional Mapping of the Human Brain*. 8th International Conference on Functional Mapping of the Human Brain, Sendai, Japan. https://matthew.dynevor.org/research/abstracts/marsbar/marsbar_abstract.pdf

Chan, Y.-C., Chou, T.-L., Chen, H.-C., & Liang, K.-C. (2012). Segregating the comprehension and elaboration processing of verbal jokes: An fMRI study. *NeuroImage*, *61*(4), 899–906.

Chan, Y.-C., Chou, T.-L., Chen, H.-C., Yeh, Y.-C., Lavallee, J. P., Liang, K.-C., & Chang, K.-E. (2013). Towards a neural circuit model of verbal humor processing: an fMRI study of the neural substrates of incongruity detection and resolution. *NeuroImage*, *66*, 169–176.

Chan, Y.-C., Zeitlen, D. C., & Beaty, R. E. (2023). Amygdala-frontoparietal effective connectivity in creativity and humor processing. *Human Brain Mapping*, *44*(6), 2585–2606.

Chang, C.-Y., Chan, Y.-C., & Chen, H.-C. (2023). Verification of the four-stage model of humor processing: Evidence from an fMRI study by three-element verbal jokes. *Brain Sciences*, *13*(3), 417.

Cherones, T. (1992, November 25). *The Airport* [Television]. NBC.

Cherones, T. (1993, January 6). *The Movie* [Television]. NBC.

Cox, R. W., & Hyde, J. S. (1997). Software tools for analysis and visualization of fMRI data. *NMR in Biomedicine*, *10*(4–5), 171–178.

Crinion, J., Turner, R., Grogan, A., Hanakawa, T., Noppeney, U., Devlin, J. T., Aso, T., Urayama, S., Fukuyama, H., Stockton, K., Usui, K., Green, D. W., & Price, C. J. (2006). Language control in the bilingual brain. *Science*, *312*(5779), 1537–1540.

Caruana, F., Avanzini, P., Gozzo, F., Francione, S., Cardinale, F., & Rizzolatti, G. (2015). Mirth and laughter elicited by electrical stimulation of the human anterior cingulate cortex. *Cortex; a Journal Devoted to the Study of the Nervous System and Behavior*, *71*, 323–331. https://doi.org/10.1016/j.cortex.2015.07.024

Dale, A. M., Fischl, B., & Sereno, M. I. (1999). Cortical Surface-Based Analysis: I. Segmentation and Surface Reconstruction. *NeuroImage*, *9*(2), 179–194.

Darvas, M., Henschen, C. W., & Palmiter, R. D. (2014). Contributions of signaling by dopamine neurons in dorsal striatum to cognitive behaviors corresponding to those observed in Parkinson's disease. *Neurobiology of Disease*, *65*, 112–123.

de la Fuente-Fernández, R., Phillips, A. G., Zamburlini, M., Sossi, V., Calne, D. B., Ruth, T. J., & Stoessl, A. J. (2002). Dopamine release in human ventral striatum and expectation of reward. *Behavioural Brain Research*, *136*(2), 359–363.

Dienes, Z. (2014). Using Bayes to get the most out of non-significant results. *Frontiers in Psychology*, *5*, 781.

Esteban, O., Blair, R., Markiewicz, C. J., Berleant, S. L., Moodie, C., Ma, F., Isik, A. I., Erramuzpe, A., Kent James D. andGoncalves, M., DuPre, E., Sitek, K. R., Gomez, D. E.

P., Lurie, D. J., Ye, Z., Poldrack, R. A., & Gorgolewski, K. J. (2018). fMRIPrep. *Software: Practice & Experience*. https://doi.org/10.5281/zenodo.852659

Esteban, O., Markiewicz, C., Blair, R. W., Moodie, C., Isik, A. I., Erramuzpe Aliaga, A., Kent, J., Goncalves, M., DuPre, E., Snyder, M., Oya, H., Ghosh, S., Wright, J., Durnez, J., Poldrack, R., & Gorgolewski, K. J. (2018). fMRIPrep: a robust preprocessing pipeline for functional MRI. *Nature Methods*. https://doi.org/10.1038/s41592-018-0235-4

Farkas, A. H., Trotti, R. L., Edge, E. A., Huang, L.-Y., Kasowski, A., Thomas, O. F., Chlan, E., Granros, M. P., Patel, K. K., & Sabatinelli, D. (2021). Humor and emotion: Quantitative meta analyses of functional neuroimaging studies. *Cortex; a Journal Devoted to the Study of the Nervous System and Behavior*, *139*, 60–72.

Fiacconi, C. M., & Owen, A. M. (2015). Using psychophysiological measures to examine the temporal profile of verbal humor elicitation. *PloS One*, *10*(8), e0135902.

Filik, R., Ţurcan, A., Ralph-Nearman, C., & Pitiot, A. (2019). What is the difference between irony and sarcasm? An fMRI study. *Cortex; a Journal Devoted to the Study of the Nervous System and Behavior*, *115*, 112–122.

Filimon, F., Nelson, J. D., Sejnowski, T. J., Sereno, M. I., & Cottrell, G. W. (2020). The ventral striatum dissociates information expectation, reward anticipation, and reward receipt. *Proceedings of the National Academy of Sciences of the United States of America*, *117*(26), 15200–15208.

Fonov, V. S., Evans, A. C., McKinstry, R. C., Almli, C. R., & Collins, D. L. (2009). Unbiased nonlinear average age-appropriate brain templates from birth to adulthood. *NeuroImage*, *47, Supplement 1*, S102.

Glasser, M. F., Sotiropoulos, S. N., Wilson, J. A., Coalson, T. S., Fischl, B., Andersson, J. L., Xu, J., Jbabdi, S., Webster, M., Polimeni, J. R., Van Essen, D. C., & Jenkinson, M. (2013). The minimal preprocessing pipelines for the Human Connectome Project. *NeuroImage*, *80*, 105–124.

Goel, V., & Dolan, R. J. (2001). The functional anatomy of humor: Segregating cognitive and affective components. *Nature Neuroscience*, *4*(3), 237–238.

Goldin, P. R., Hutcherson, C. A. C., Ochsner, K. N., Glover, G. H., Gabrieli, J. D. E., & Gross, J. J. (2005). The neural bases of amusement and sadness: A comparison of block contrast and subject-specific emotion intensity regression approaches. *NeuroImage*, *27*(1), 26–36.

Gorgolewski, K. J., Burns, C. D., Madison, C., Clark, D., Halchenko, Y. O., Waskom, M. L., & Ghosh, S. (2011). Nipype: a flexible, lightweight and extensible neuroimaging data processing framework in Python. *Frontiers in Neuroinformatics*, *5*, 13.

Gorgolewski, K. J., Esteban, O., Markiewicz, C. J., Ziegler, E., Ellis, D. G., Notter, M. P., Jarecka, D., Johnson, H., Burns, C., Manhães-Savio, A., Hamalainen, C., Yvernault, B., Salo, T., Jordan, K., Goncalves, M., Waskom, M., Clark, D., Wong, J., Loney, F., … Ghosh, S. (2018). Nipype. *Software: Practice & Experience*. https://doi.org/10.5281/zenodo.596855

Graff-Radford, J., Williams, L., Jones, D. T., & Benarroch, E. E. (2017). Caudate nucleus as a component of networks controlling behavior. *Neurology*, *89*(21), 2192–2197.

Greve, D. N., & Fischl, B. (2009). Accurate and robust brain image alignment using boundary-based registration. *NeuroImage*, *48*(1), 63–72.

Haber, S. N. (2016). Corticostriatal circuitry. *Dialogues in Clinical Neuroscience*, *18*(1), 7–21.

Hiebert, N. M., Owen, A. M., Ganjavi, H., Mendonça, D., Jenkins, M. E., Seergobin, K. N., & MacDonald, P. A. (2019). Dorsal striatum does not mediate feedback-based, stimulus-response learning: An event-related fMRI study in patients with Parkinson's disease tested on and off dopaminergic therapy. *NeuroImage*, *185*, 455–470.

Iwase, M., Ouchi, Y., Okada, H., Yokoyama, C., Nobezawa, S., Yoshikawa, E., Tsukada, H., Takeda, M., Yamashita, K., Takeda, M., Yamaguti, K., Kuratsune, H., Shimizu, A., & Watanabe, Y. (2002). Neural substrates of human facial expression of pleasant emotion induced by comic films: A PET study. *NeuroImage*, *17*(2), 758–768.

Jeffreys, H. (1939). *The Theory of Probability*.

Jenkinson, M., Bannister, P., Brady, M., & Smith, S. (2002). Improved Optimization for the Robust and Accurate Linear Registration and Motion Correction of Brain Images. *NeuroImage*, *17*(2), 825–841.

Keysers, C., Gazzola, V., & Wagenmakers, E.-J. (2020). Using Bayes factor hypothesis testing in neuroscience to establish evidence of absence. *Nature Neuroscience*, *23*(7), 788–799.

Kipman, M., Weber, M., Schwab, Z. J., DelDonno, S. R., & Killgore, W. D. S. (2012). A funny thing happened on the way to the scanner: Humor detection correlates with gray matter volume. *Neuroreport*, *23*(18), 1059–1064.

Kireev, M. V., Medvedeva, N. S., Korotkov, A. D., & Medvedev, S. V. (2015). Functional interactions between the caudate nuclei and inferior frontal gyrus providing deliberate deception. *Human Physiology*, *41*(1), 22–26.

Klein, A., Ghosh, S. S., Bao, F. S., Giard, J., Häme, Y., Stavsky, E., Lee, N., Rossa, B., Reuter, M., Neto, E. C., & Keshavan, A. (2017). Mindboggling morphometry of human brains. *PLoS Computational Biology*, *13*(2), e1005350.

Knutson, B., Adams, C. M., Fong, G. W., & Hommer, D. (2001). Anticipation of increasing monetary reward selectively recruits nucleus accumbens. *The Journal of Neuroscience: The Official Journal of the Society for Neuroscience*, *21*(16), RC159.

Lanczos, C. (1964). Evaluation of Noisy Data. *Journal of the Society for Industrial and Applied Mathematics Series B Numerical Analysis*, *1*(1), 76–85.

Lewis, S. J. G., Dove, A., Robbins, T. W., Barker, R. A., & Owen, A. M. (2004). Striatal contributions to working memory: A functional magnetic resonance imaging study in humans. *The European Journal of Neuroscience*, *19*(3), 755–760.

MacDonald, P. A., & Monchi, O. (2011). Differential effects of dopaminergic therapies on dorsal and ventral striatum in Parkinson’s disease: Implications for cognitive function. *Parkinson’s Disease*, *2011*, 572743.

Mensen, A., Poryazova, R., Schwartz, S., & Khatami, R. (2014). Humor as a reward mechanism: Event-related potentials in the healthy and diseased brain. *PloS One*, *9*(1), e85978.

Mestres-Missé, A., Turner, R., & Friederici, A. D. (2012). An anterior-posterior gradient of cognitive control within the dorsomedial striatum. *NeuroImage*, *62*(1), 41–47.

Mobbs, D., Greicius, M. D., Abdel-Azim, E., Menon, V., & Reiss, A. L. (2003). Humor modulates the mesolimbic reward centers. *Neuron*, *40*(5), 1041–1048.

Mobbs, D., Hagan, C. C., Azim, E., Menon, V., & Reiss, A. L. (2005). Personality predicts activity in reward and emotional regions associated with humor. *Proceedings of the National Academy of Sciences of the United States of America*, *102*(45), 16502–16506.

Moran, J. M., Wig, G. S., Adams, R. B., Jr, Janata, P., & Kelley, W. M. (2004). Neural correlates of humor detection and appreciation. *NeuroImage*, *21*(3), 1055–1060.

Neely, M. N., Walter, E., Black, J. M., & Reiss, A. L. (2012). Neural correlates of humor detection and appreciation in children. *The Journal of Neuroscience: The Official Journal of the Society for Neuroscience*, *32*(5), 1784–1790.

Nichols, T., Brett, M., Andersson, J., Wager, T., & Poline, J.-B. (2005). Valid conjunction inference with the minimum statistic [Review of *Valid conjunction inference with the minimum statistic*]. *NeuroImage*, *25*(3), 653–660. https://doi.org/10.1016/j.neuroimage.2004.12.005

Noh, J., Seok, J.-W., Kim, S.-H., Cheong, C., & Sohn, J.-H. (2014). Neural substrates associated with humor processing. *Journal of Analytical Science and Technology*, *5*(1), 1–6.

Osaka, M., Yaoi, K., Minamoto, T., & Osaka, N. (2014). Serial changes of humor comprehension for four-frame comic Manga: an fMRI study. *Scientific Reports*, *4*, 5828.

Palejwala, A. H., Dadario, N. B., Young, I. M., O'Connor, K., Briggs, R. G., Conner, A. K., O'Donoghue, D. L., & Sughrue, M. E. (2021). Anatomy and white matter connections of the lingual gyrus and cuneus. *World Neurosurgery*, *151*, e426–e437. https://doi.org/10.1016/j.wneu.2021.04.050

Pool, E. R., Munoz Tord, D., Delplanque, S., Stussi, Y., Cereghetti, D., Vuilleumier, P., & Sander, D. (2022). Differential contributions of ventral striatum subregions to the motivational and hedonic components of the affective processing of reward. *The Journal of Neuroscience: The Official Journal of the Society for Neuroscience*, *42*(13), 2716–2728.

Postuma, R. B., & Dagher, A. (2006). Basal ganglia functional connectivity based on a meta-analysis of 126 positron emission tomography and functional magnetic resonance imaging publications. *Cerebral Cortex* , *16*(10), 1508–1521.

Power, J. D., Mitra, A., Laumann, T. O., Snyder, A. Z., Schlaggar, B. L., & Petersen, S. E. (2014). Methods to detect, characterize, and remove motion artifact in resting state fMRI. *NeuroImage*, *84*(Supplement C), 320–341.

Prenger, M., Van Hedger, K., Seergobin, K. N., Owen, A., & MacDonald, P. A. (under review). Parkinson's disease impairs humor comprehension, but not appreciation. *Journal of Parkinson's Disease*.

R Core Team. (2022). *R: A language and environment for statistical computing* (4.2.0) [MacOS]. R Foundation for Statistical Computing. https://www.R-project.org/

Rolls, E. T., Huang, C.-C., Lin, C.-P., Feng, J., & Joliot, M. (2020). Automated anatomical labelling atlas 3. *NeuroImage*, *206*, 116189.

Rorden, C., & Brett, M. (2000). Stereotaxic display of brain lesions. *Behavioural Neurology*, *12*(4), 191–200.

RStudio Team. (2022). *RStudio: Integrated Development for R* (2022.07.01) [MacOS]. http://www.rstudio.com/

Samson, A. C., Hempelmann, C. F., Huber, O., & Zysset, S. (2009). Neural substrates of incongruity-resolution and nonsense humor. *Neuropsychologia*, *47*(4), 1023–1033.

Samson, A. C., Zysset, S., & Huber, O. (2008). Cognitive humor processing: Different logical mechanisms in nonverbal cartoons: An fMRI study. *Social Neuroscience*, *3*(2), 125–140.

Sanz-Arigita, E., Daviaux, Y., Joliot, M., Dilharreguy, B., Micoulaud-Franchi, J.-A., Bioulac, S., Taillard, J., Philip, P., & Altena, E. (2021). Brain reactivity to humorous films is affected by insomnia. *Sleep*, *44*(9). https://doi.org/10.1093/sleep/zsab081

Satow, T., Usui, K., Matsuhashi, M., Yamamoto, J., Begum, T., Shibasaki, H., Ikeda, A., Mikuni, N., Miyamoto, S., & Hashimoto, N. (2003). Mirth and laughter arising from human temporal cortex. *Journal of Neurology, Neurosurgery, and Psychiatry*, *74*(7), 1004–1005.

Satterthwaite, T. D., Elliott, M. A., Gerraty, R. T., Ruparel, K., Loughead, J., Calkins, M. E., Eickhoff, S. B., Hakonarson, H., Gur, R. C., Gur, R. E., & Wolf, D. H. (2013). An improved framework for confound regression and filtering for control of motion artifact in the preprocessing of resting-state functional connectivity data. *NeuroImage*, *64*(1), 240–256.

Schultz, W. (2016). Dopamine reward prediction error coding. *Dialogues in Clinical Neuroscience*, *18*(1), 23–32.

Shibata, M., Terasawa, Y., & Umeda, S. (2014). Integration of cognitive and affective networks in humor comprehension. *Neuropsychologia*, *65*, 137–145.

Suls, J. M. (1972). A Two-Stage Model for the Appreciation of Jokes and Cartoons: An Information-Processing Analysis. In J. H. Goldstein & P. E. McGhee (Eds.), *The Psychology of Humor* (pp. 81–100). Academic Press.

Swash, M. (1972). Released involuntary laughter after temporal lobe infarction. *Journal of Neurology, Neurosurgery, and Psychiatry*, *35*(1), 108–113.

Thaler, A., Posen, J., Giladi, N., Manor, Y., Mayanz, C., Mirelman, A., & Gurevich, T. (2012). Appreciation of humor is decreased among patients with Parkinson's disease. *Parkinsonism & Related Disorders*, *18*(2), 144–148.

The Mathworks Inc. (2022). *MATLAB* (9.12.0 (R2022a)) [Computer software].

Tustison, N. J., Avants, B. B., Cook, P. A., Zheng, Y., Egan, A., Yushkevich, P. A., & Gee, J. C. (2010). N4ITK: Improved N3 Bias Correction. *IEEE Transactions on Medical Imaging*, *29*(6), 1310–1320.

Viñas-Guasch, N., & Wu, Y. J. (2017). The role of the putamen in language: A meta-analytic connectivity modeling study. *Brain Structure & Function*, *222*(9), 3991–4004.

Vrticka, P., Black, J. M., & Reiss, A. L. (2013). The neural basis of humour processing. *Nature Reviews. Neuroscience*, *14*(12), 860–868.

Watson, K. K., Matthews, B. J., & Allman, J. M. (2007). Brain activation during sight gags and language-dependent humor. *Cerebral Cortex* , *17*(2), 314–324.

Wellcome Department of Imaging Neuroscience. (2014). *Statistical Parametric Mapping* (Version 12) [Computer software].

Wild, B., Rodden, F. A., Rapp, A., Erb, M., Grodd, W., & Ruch, W. (2006). Humor and smiling: Cortical regions selective for cognitive, affective, and volitional components. *Neurology*, *66*(6), 887–893.

Wildgruber, D., Szameitat, D. P., Ethofer, T., Brück, C., Alter, K., Grodd, W., & Kreifelts, B. (2013). Different types of laughter modulate connectivity within distinct parts of the laughter perception network. *PloS One*, *8*(5), e63441.

World Medical Association. (2013). World Medical Association Declaration of Helsinki: Ethical principles for medical research involving human subjects. *JAMA: The Journal of the American Medical Association*, *310*(20), 2191–2194.

Yamao, Y., Matsumoto, R., Kunieda, T., Shibata, S., Shimotake, A., Kikuchi, T., Satow, T., Mikuni, N., Fukuyama, H., Ikeda, A., & Miyamoto, S. (2015). Neural correlates of mirth and laughter: A direct electrical cortical stimulation study. *Cortex; a Journal Devoted to the Study of the Nervous System and Behavior*, *66*, 134–140.

Zandbelt, B. B., & Vink, M. (2010). On the role of the striatum in response inhibition. *PloS One*, *5*(11), e13848.

Zhang, Y., Brady, M., & Smith, S. (2001). Segmentation of brain MR images through a hidden Markov random field model and the expectation-maximization algorithm. *IEEE Transactions on Medical Imaging*, *20*(1), 45–57.

Ziv, A. (1984). *Personality and Sense of Humor*. Springer Publishing Co.

List of Figures

Figure 1: fMRI humor processing task. Participants listened to joke and non-joke audio clips ranging from 3-13 sec in length. Following this, they were asked to categorize the audio clip as either a joke or a non-joke. Next, they were asked to rate how funny the audio clip was, regardless of whether it was a joke or not and regardless of their previous response. Participants used an MRI-safe button box to move their selection (in green) up or down and confirm their response. Each response screen timed out if a response was not made after 5000 msec. Inter-trial and inter-response intervals were jittered with variable durations sampled from an exponential distribution (min = 525 msec; mean = 2500 msec; max = 7000 msec).

Figure 2: Dorsal (blue) and ventral (green) striatum regions of interest, delineated by z = 2 mm in MNI space.

Figure 3: *Seinfeld*-viewing task events are shown on a representative waveform. Humor comprehension events were defined as the two seconds prior to the onset of laughter in the episode laugh track (blue). Humor appreciation events were defined as the middle two seconds of laughter in the laugh track (green). Control events were defined as the two second epochs directly between neighboring comprehension and appreciation events (magenta).

Figure 4: Conjunction analysis for humor comprehension (warm colors) and appreciation (cool colors) contrasts across tasks. Color bars represent *t*-values.

Figure 5: Significant activation was observed in the dorsal striatum (DS) and the ventral striatum (VS) during the Joke > Non-Joke contrast for correct trials only, a measure of humor comprehension **(A)**. Significant activation was observed in the VS, but not the DS, during the

Funny > Not Funny contrast for all trials, a measure of humor appreciation **(B)**. a.u. = arbitrary units. *p < 0.05, **p < 0.01

Figure 6: Significant activation was observed in the dorsal striatum (DS) and the ventral striatum (VS) during the Joke > Non-Joke contrast for correct trials only, a measure of humor comprehension **(A)**. Significant activation was observed in the VS, but not the DS, during the Funny > Not Funny contrast for all trials, a measure of humor appreciation **(B)**. a.u. = arbitrary units. *p < 0.05, **p < 0.01

List of Tables

Table 1: Seinfeld-viewing task post-scan questionnaire data

Data are presented as absolute values and percentage of sample in parentheses, except where indicated. Statistically significant differences are indicated by asterisks (*$p < 0.05$, **$p < 0.01$, ***$p < 0.001$).

Table 2: Whole-brain BOLD activation in the Joke Task for Humor Comprehension (Joke > Non-Joke Contrast)

MNI coordinates, *t*-values, and *p*-values represent that of the peak voxel within each cluster, defined by a voxel-level FWE-corrected height threshold of $p < 0.05$ and a cluster-level extent threshold of $k = 10$. Anatomical regions represent the location of the peak voxel, identified using the automated anatomical labelling atlas version 3 (AAL3). Clusters that include striatal or midbrain structures are presented with †. BA = Brodmann area; R = right; L = left.

Table 3: Whole-brain BOLD Activation in the Joke Task for Humor Appreciation (Funny > Not Funny Contrast)

MNI coordinates, *t*-values, and *p*-values represent that of the peak voxel within each cluster, defined by a voxel-level FWE-corrected height threshold of $p < 0.05$ and a cluster-level extent threshold of $k = 10$. Anatomical regions represent the location of the peak voxel, identified using the automated anatomical labelling atlas version 3 (AAL3). Clusters that include striatal or midbrain structures are presented with †. BA = Brodmann area; R = right; L = left.

Table 4: Whole-brain BOLD Activation in the *Seinfeld*-viewing Task for Humor Comprehension

MNI coordinates, *t*-values, and *p*-values represent that of the peak voxel within each cluster, defined by a voxel-level FWE-corrected height threshold of $p < 0.05$ and a cluster-level extent threshold of $k = 10$. Anatomical regions represent the location of the peak voxel, identified using the automated anatomical labelling atlas version 3 (AAL3). Clusters that include striatal or midbrain structures are presented with †. BA = Brodmann area; R = right; L = left.

Table 5: Whole-brain BOLD Activation in the *Seinfeld*-viewing Task for Humor Appreciation

MNI coordinates, *t*-values, and *p*-values represent that of the peak voxel within each cluster, defined by a voxel-level FWE-corrected height threshold of $p < 0.05$ and a cluster-level extent threshold of $k = 10$. Anatomical regions represent the location of the peak voxel, identified using the automated anatomical labelling atlas version 3 (AAL3). Clusters that include striatal or midbrain structures are presented with †. BA = Brodmann area; R = right; L = left.

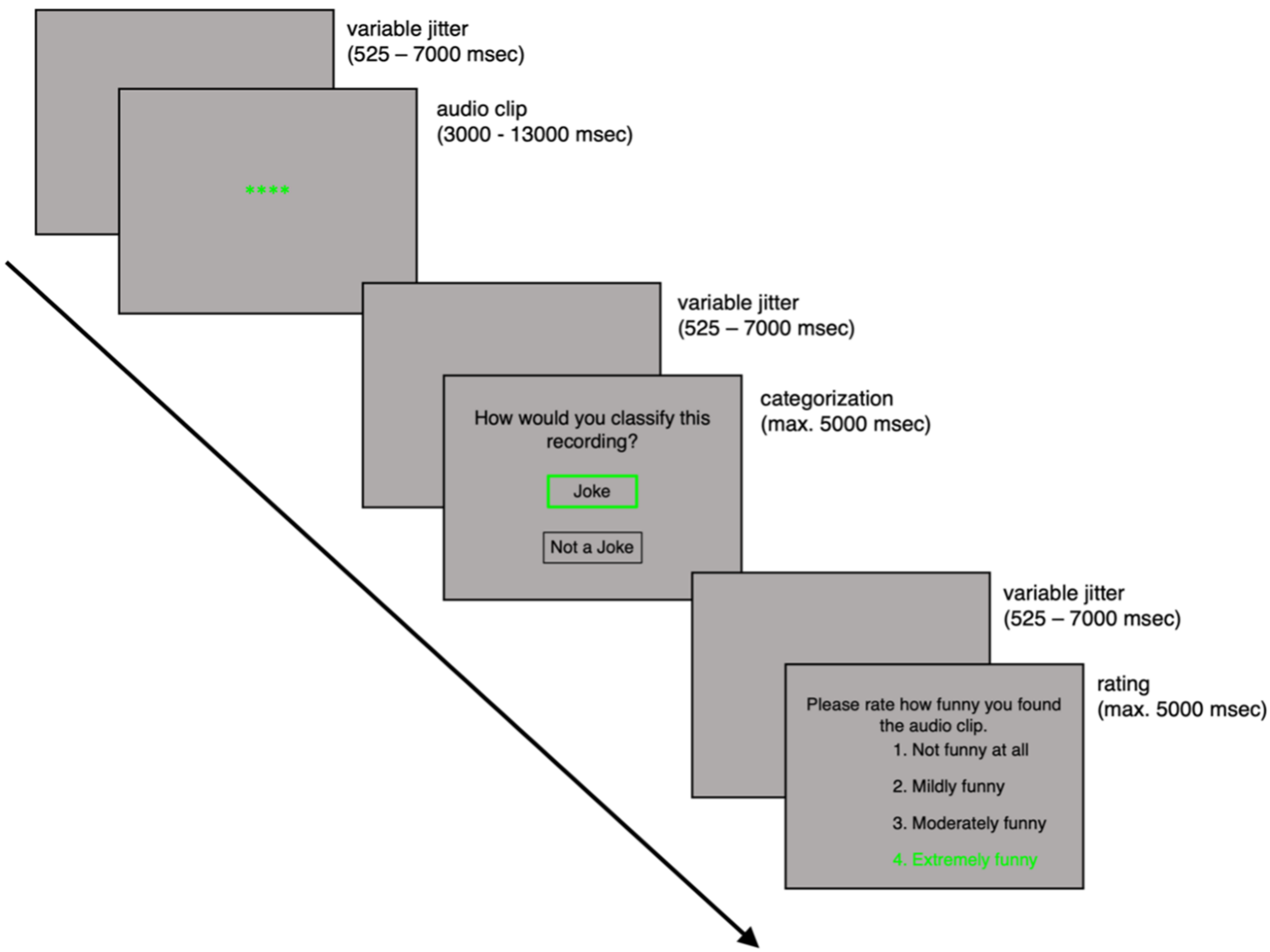
variable jitter
(525 – 7000 msec)
audio clip
(3000 - 13000 msec)
****
variable jitter
(525 – 7000 msec)
categorization
(max. 5000 msec)
How would you classify this recording?
Joke
Not a Joke
variable jitter
(525 – 7000 msec)
rating
(max. 5000 msec)
Please rate how funny you found the audio clip.
1. Not funny at all
2. Mildly funny
3. Moderately funny
4. Extremely funny

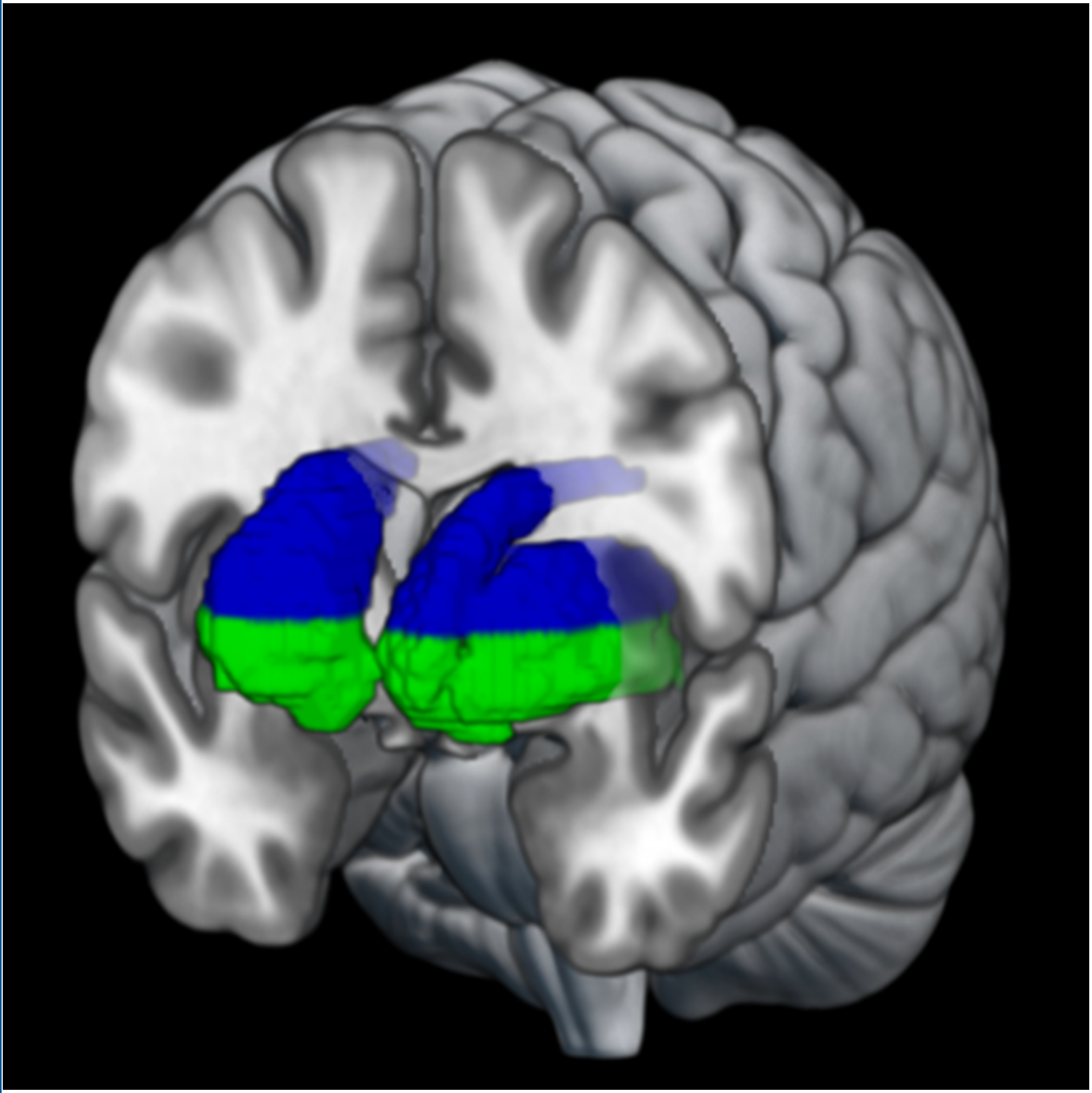

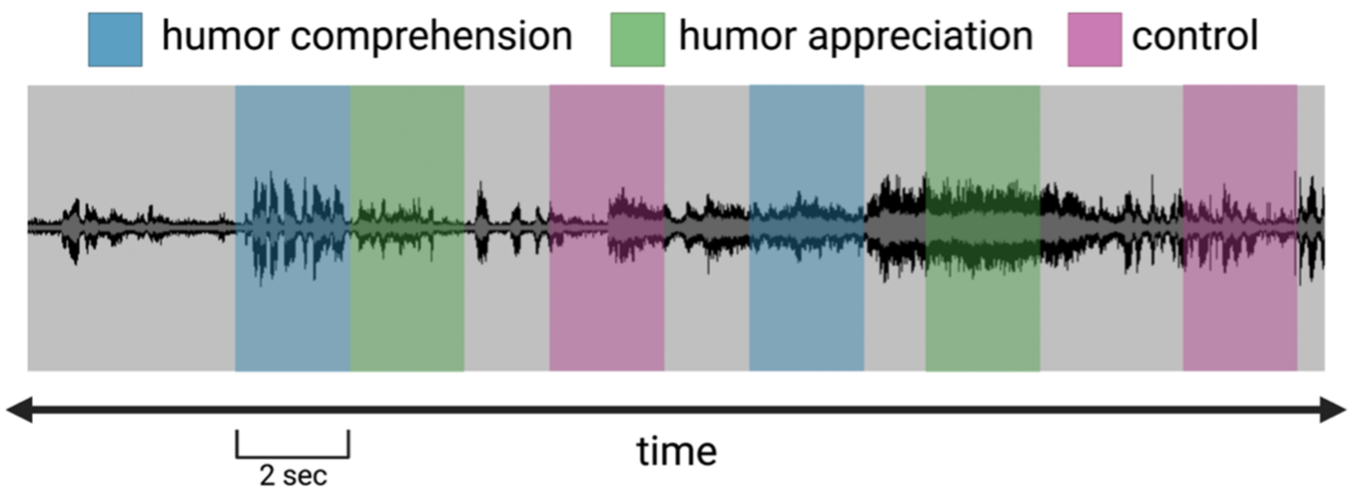
humor comprehension
humor appreciation
control
2 sec
time

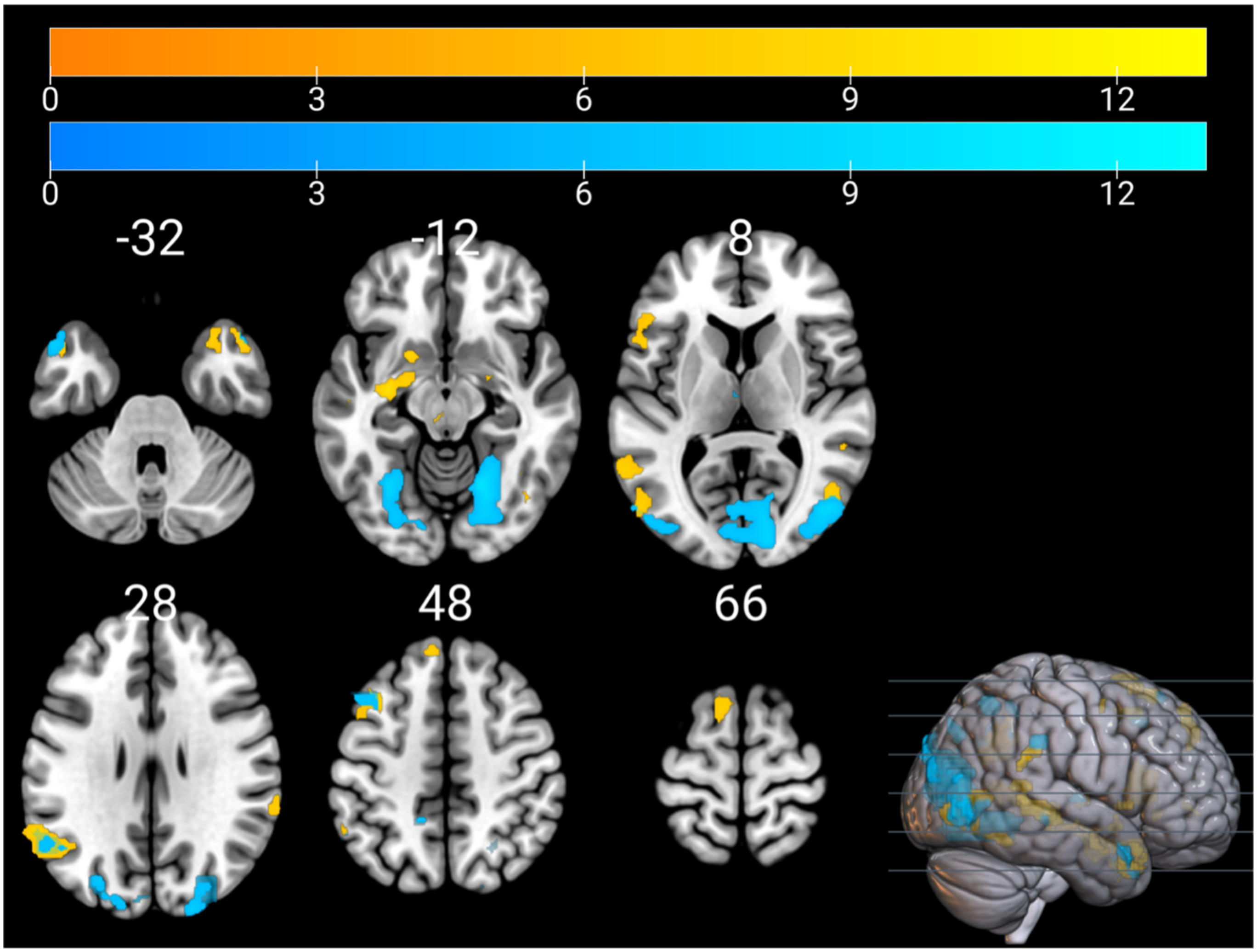
0
3
6
9
12
0
3
6
9
12
-32
-12
8
28
48
66

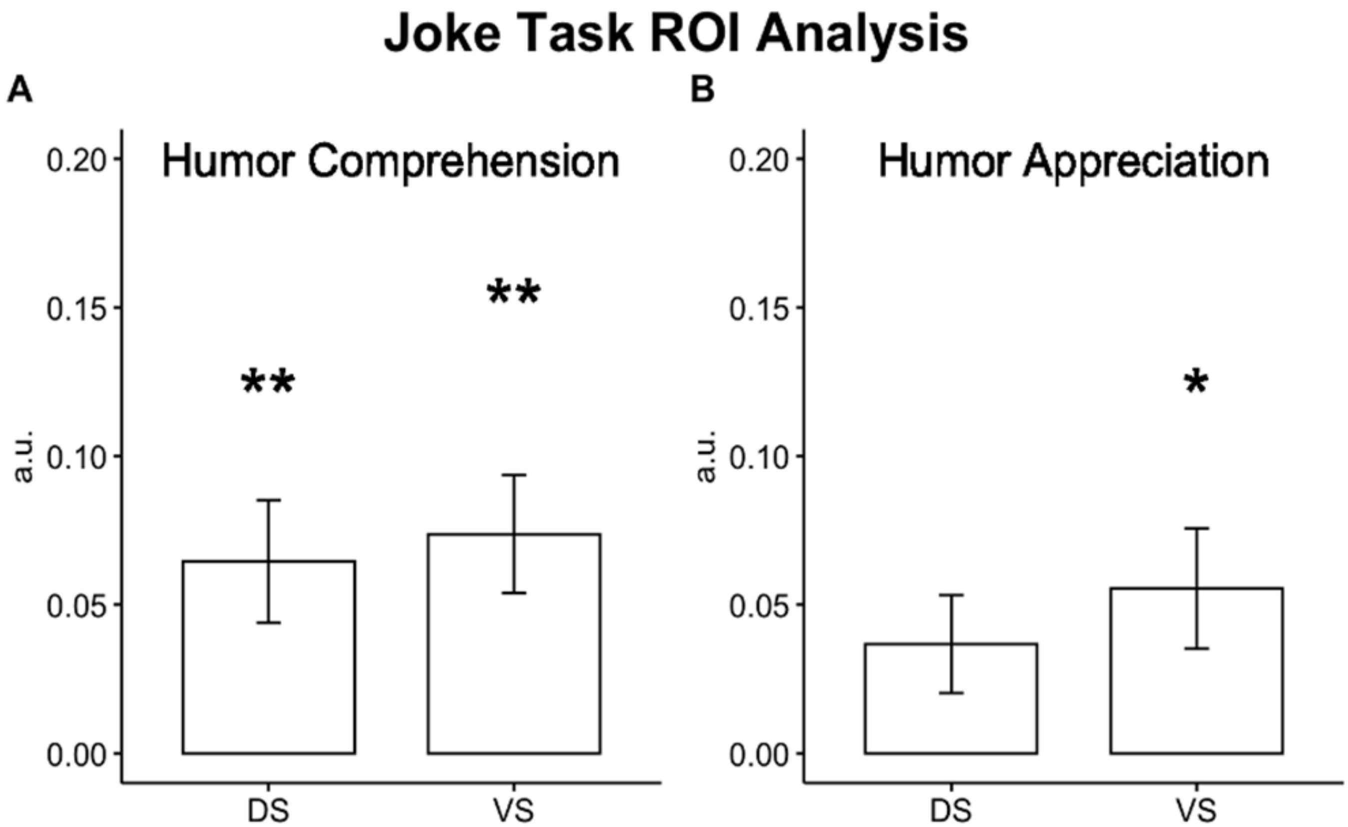

Joke Task ROI Analysis
A
B
Humor Comprehension
Humor Appreciation
0.20
0.15
0.10
0.05
0.00
a.u.
**
**
*
DS
VS

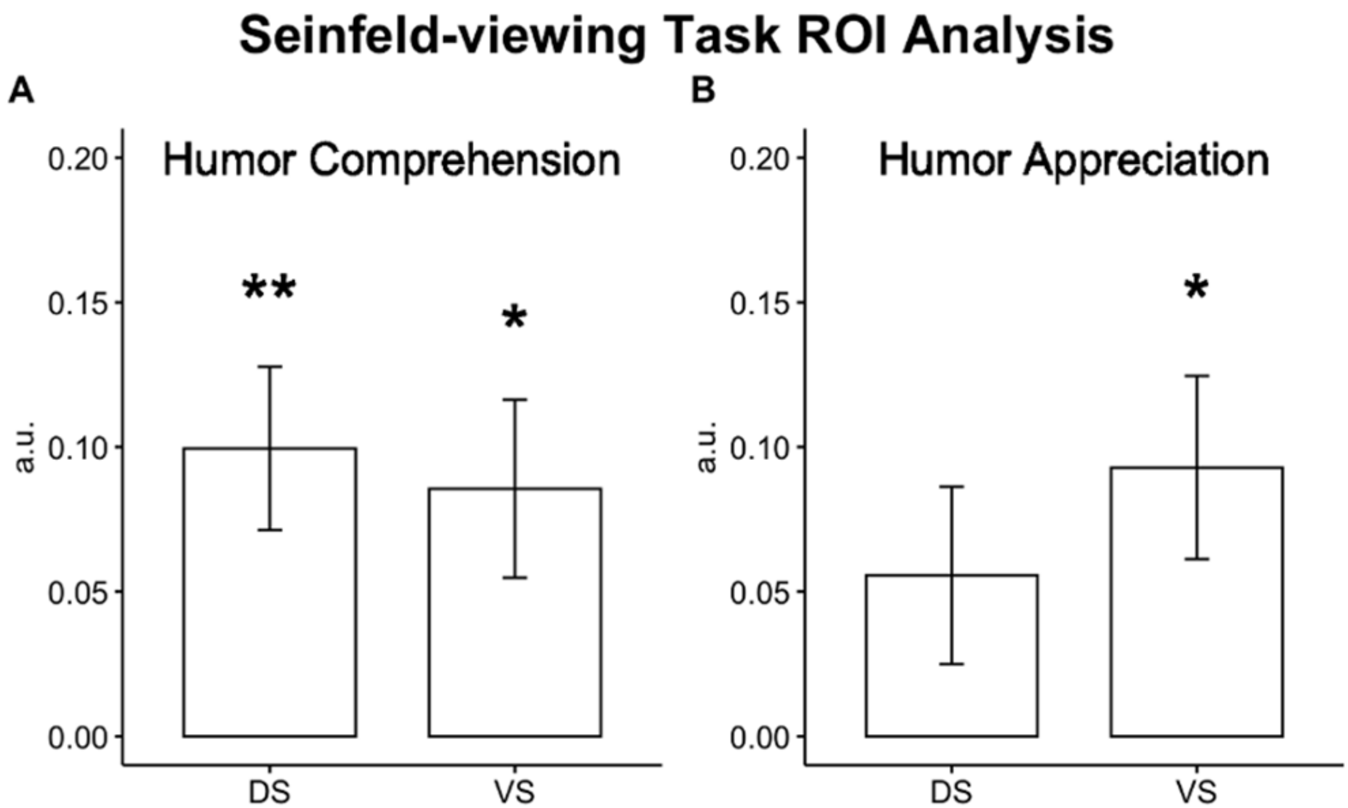

Seinfeld-viewing Task ROI Analysis
A
B
Humor Comprehension
Humor Appreciation
**
*
*
a.u.
0.20
0.15
0.10
0.05
0.00
DS
VS

Table 1: Seinfeld-viewing task post-scan questionnaire data

	S4E12, The Airport (n = 13)	**S4E14, *The Movie* (n = 13)**	**Overall (N = 26)**
How familiar are you with *Seinfeld*?			
I had never watched an episode of *Seinfeld* previously	5 (38 %)	6 (46 %)	11 (42 %)
I had watched a few episodes here and there, but never a full season	8 (62 %)	3 (23 %)	11 (42 %)
I have watched at least one season but not the entire series	0 (0 %)	2 (15 %)	2 (8 %)
I have watched the entire series once	0 (0 %)	1 (8 %)	1 (4 %)
I have watched the entire series multiple times	0 (0 %)	1 (8 %)	1 (4 %)
Average time since last watching *Seinfeld*? (# of days)			
Mean (SD)	497.63 (± 607.13)	505.57 (± 695.32)	501.33 (± 625.72)
Not applicable (i.e., I've never watched *Seinfeld* before)	5 (38.5%)	6 (46.2%)	11 (42.3%)
How frequently do you watch sitcoms, in general? (# of episodes per month)			
Never (0 per month)	2 (15 %)	4 (31 %)	6 (23 %)
Sometimes (1-5 per month)	4 (31 %)	3 (23 %)	7 (27 %)
Often (5-10 per month)	2 (15 %)	1 (8 %)	3 (12 %)

	S4E12, The Airport (n = 13)	S4E14, *The Movie* (n = 13)	Overall (N = 26)
Very Often (10-15 per month)	0 (0 %)	0 (0 %)	0 (0 %)
Always (15+ per month)	5 (38 %)	5 (38 %)	10 (38 %)
Have you ever seen this episode of *Seinfeld* before?			
No	13 (100 %)	12 (92 %)	25 (96 %)
Yes	0 (0 %)	1 (8 %)	1 (4 %)
How funny was this episode of *Seinfeld*, from 1(not funny at all) to 10 (funniest thing I've seen in my life)?			
Mean (SD)	4.46 (± 2.15)	5.31 (± 1.49)	4.88 (± 1.86)

Data are presented as absolute values and percentage of sample in parentheses, except where indicated. Statistically significant differences are indicated by asterisks (*$p < 0.05$, **$p < 0.01$, ***$p < 0.001$).

Table 2: Whole-brain BOLD activation in the Joke Task for Humor Comprehension (Joke > Non-Joke Contrast)

Anatomical Region	**Coordinates [X Y Z]**	**Cluster Size (k_E)**	***t*-value**	$p_{\text{FWE-corr}}$
R Middle Temporal Gyrus (BA 21)	49 -30 -3	215	12.71	< 0.001
L Temporal Pole (BA 38)	-48 13 -30	114	9.93	< 0.001
L Middle Frontal Gyrus (BA 8)	-34 16 50	113	9.52	< 0.001
L Angular Gyrus	-51 -60 30	414	8.92	< 0.001
L Inferior Frontal Gyrus (pars triangularis)	-51 18 17	223	8.83	< 0.001
L Middle Temporal Gyrus	-61 -52 10	319	8.74	< 0.001
L Putamen†	-18 6 -10	82	8.74	< 0.001
L Superior Frontal Gyrus	-6 43 47	100	8.36	.001
R Temporal Pole	49 13 -33	93	8.29	.001
L Supplementary Motor Area (BA 6)	-8 13 67	150	7.97	.001
L Midbrain†	-4 -27 2	112	7.89	.001
L Inferior Frontal Gyrus (pars triangularis; BA 10)	-51 46 0	30	7.56	.003
L Thalamus	-4 -12 4	31	7.44	.004

MNI coordinates, *t*-values, and *p*-values represent that of the peak voxel within each cluster, defined by a voxel-level FWE-corrected height threshold of $p < 0.05$ and a cluster-level extent threshold of $k = 10$. Anatomical regions represent the location of the peak voxel, identified using the automated anatomical labelling atlas version 3 (AAL3). Clusters that include striatal or midbrain structures are presented with †. BA = Brodmann area; R = right; L = left.

Table 3: Whole-brain BOLD Activation in the Joke Task for Humor Appreciation (Funny > Not Funny Contrast)

Anatomical Region	**Coordinates [X Y Z]**	**Cluster Size (k_E)**	***t*-value**	$p_{\text{FWE-corr}}$
L Temporal Pole (BA 38)	-51 13 -28	77	9.12	< 0.001
L Middle Frontal Gyrus	-38 18 44	52	7.93	.001
R Temporal Pole	54 10 -23	31	7.41	.003
L Angular Gyrus	-54 -60 32	154	7.41	.004
L Thalamus	-1 -14 4	13	7.25	.005
R Middle Temporal Gyrus	49 -32 -6	29	7.25	.005
L Superior Frontal Gyrus	-8 28 57	10	6.89	.011
L Middle Temporal Gyrus	-58 -30 -6	15	6.49	.025

MNI coordinates, *t*-values, and *p*-values represent that of the peak voxel within each cluster, defined by a voxel-level FWE-corrected height threshold of $p < 0.05$ and a cluster-level extent threshold of $k = 10$. Anatomical regions represent the location of the peak voxel, identified using the automated anatomical labelling atlas version 3 (AAL3). Clusters that include striatal or midbrain structures are presented with †. BA = Brodmann area; R = right; L = left.

Table 4: Whole-brain BOLD Activation in the *Seinfeld*-viewing Task for Humor Comprehension

Anatomical Region	**Coordinates [X Y Z]**	**Cluster Size (k_E)**	***t*-value**	$p_{FWE\text{-}corr}$
R Middle Temporal Gyrus (BA 37)	49 -72 2	399	10.47	< 0.001
L Hippocampus	-31 -10 -13	367	10.12	< 0.001
R Temporal Pole (BA 38)	32 18 -33	145	8.93	< 0.001
L Middle Temporal Gyrus	-51 -70 7	100	8.26	.001
R Supramarginal Gyrus	64 -27 30	80	7.71	.002
R Superior Temporal Gyrus	49 -42 12	61	7.67	.003
R Amygdala	22 -4 -16	66	7.64	.003
L Fusiform Gyrus	-41 -52 -18	14	7.60	.003
R Insula	36 8 2	36	7.57	.003
L Midbrain[†]	-1 -37 -3	12	7.48	.004
L Inferior Frontal Gyrus (pars orbicularis)	-44 28 -3	24	7.45	.004
L Insula	-38 6 2	13	7.17	.007
R Middle Frontal Gyrus (BA6)	42 0 54	24	7.14	.007
R Supplementary Motor Area	2 16 62	29	6.85	.013

MNI coordinates, t-values, and p-values represent that of the peak voxel within each cluster, defined by a voxel-level FWE-corrected height threshold of $p < 0.05$ and a cluster-level extent threshold of $k = 10$. Anatomical regions represent the location of the peak voxel, identified using the automated anatomical labelling atlas version 3 (AAL3). Clusters that include striatal or midbrain structures are presented with †. BA = Brodmann area; R = right; L = left.

Table 5: Whole-brain BOLD Activation in the *Seinfeld*-viewing Task for Humor Appreciation

Anatomical Region	**Coordinates [X Y Z]**	**Cluster Size (k_E)**	***t*-value**	$p_{FWE\text{-}corr}$
R Inferior Temporal Gyrus (BA 37)	52 -74 -3	2321	11.16	< 0.001
L Fusiform Gyrus	-28 -64 -8	256	10.23	< 0.001
L Precuneus	-14 -47 52	25	8.18	.001
L Cerebellum (lobule VI)	-8 -67 -8	30	7.94	.001
R Superior Parietal Lobule (BA 7)	26 -60 52	40	7.65	.003
R Supramarginal Gyrus	62 -34 32	28	6.94	.012
R Precuneus (BA 7)	19 -74 40	24	6.86	.013

MNI coordinates, *t*-values, and *p*-values represent that of the peak voxel within each cluster, defined by a voxel-level FWE-corrected height threshold of $p < 0.05$ and a cluster-level extent threshold of $k = 10$. Anatomical regions represent the location of the peak voxel, identified using the automated anatomical labelling atlas version 3 (AAL3). Clusters that include striatal or midbrain structures are presented with †. BA = Brodmann area; R = right; L = left.